Nanotoxicology, 2012; Early Online, 1–11

ISSN: 1743-5390 print / 1743-5404 online
DOI: 10.3109/17435390.2012.689880

informa
healthcare

Surfactant protein D (SP-D) alters cellular uptake of particles and nanoparticles

Michaela Kendall[1], Ping Ding[2], Rose-Marie Mackay[3], Roona Deb[3], Zofi McKenzie[3], Kevin Kendall[2], Jens Madsen[3,4], & Howard Clark[3,4]

[1]European Centre of Environment and Human Health, Peninsula College of Medicine and Dentistry, University of Exeter, Truro, Cornwall, TR1 3HD, UK, [2]Department of Chemical Engineering, University of Birmingham, Birmingham, B15 2TT, UK, [3]Child Health, Sir Henry Wellcome Laboratories, Clinical and Experimental Sciences, Faculty of Medicine, University of Southampton, Southampton General Hospital, Southampton, SO16 6YD, UK and [4]Institute for Life Sciences, University of Southampton, SO17 1BJ, UK

Abstract

Surfactant protein D (SP-D) is primarily expressed in the lungs and modulates pro- and anti-inflammatory processes to toxic challenge, maintaining lung homeostasis. We investigated the interaction between NPs and SP-D and subsequent uptake by cells involved in lung immunity. Dynamic light scattering (DLS) and scanning electron microscopy (SEM) measured NP aggregation, particle size and charge in native human SP-D (NhSP-D) and recombinant fragment SP-D (rfhSP-D). SP-D aggregated NPs, especially following the addition of calcium. Immunohistochemical analysis of A549 epithelial cells investigated the co-localization of NPs and rfhSP-D. rfhSP-D enhanced the co-localisation of NPs to epithelial A549 cells *in vitro*. NP uptake by alveolar macrophages (AMs) and lung dendritic cells (LDCs) from C57BL/6 and SP-D knock-out mice were compared. AMs and LDCs showed decreased uptake of NPs in SP-D deficient mice compared to wild-type mice. These data confirmed an interaction between SP-D and NPs, and subsequent enhanced NP uptake.

Keywords: Nanoparticles, particle characterisation, nanotoxicology, mechanistic toxicology, surfactant protein D

Introduction

A key human exposure route to nanoparticles (NPs) is via the lung. Human lungs develop under exposure to airborne particles and NPs, and experience higher exposure in urban atmospheres near combustion sources such as roads (Russell & Brunekreef 2009; Spira-Cohen et al. 2011). The lung allows nanoscale material (particles, molecules or ions) to cross cellular barriers and translocate into circulatory systems (Geiser & Kreyling 2010), where particle effects are most strongly observed (Peters et al. 1997, Peters et al. 2001; COMEAP 2010; Miller 2010). Biologically plausible mechanisms for how sub-micron particles cause cardiovascular and respiratory disease are currently being sought (Araujo & Nel 2009; Gehr et al. 2006).

The mechanistic toxicity of *insoluble* NPs remains unexplained by current models, but surface area and particle size are significant factors (Kendall et al. 2004; Oberdorster et al. 2005). A fraction of inhaled NPs deposits in the lung surfactant system, where surfactant components interact with NP surfaces (Kendall et al. 2002; Kendall 2007; Lundqvist et al. 2008). These processes do not immediately involve cells directly, but are first mediated by extracellular molecules alone and may reduce surface charge to promote agglomeration (Kendall et al. 2002, 2004, 2010b, 2010a). Surfactant protein D (SP-D) is an important component of lung surfactant, but is expressed not just in the lung but at other mucosal surfaces such as the eye and genitourinary tract (Madsen et al. 2000, Ni et al. 2005). At these environment–organism interfaces, SP-D modulates innate and adaptive immunity, including inflammatory responses to a range of inhaled pathogens (Clark et al. 2002; Wright 2005). SP-D binds carbohydrates, lipids and nucleic acids with broad specificity, to initiate phagocytosis of biological particles (Palaniyar et al. 2003; Wright 2005). In the last decade, experiments in SP-D gene knock-out ($SP\text{-}D^{-/-}$) mice and monitoring of human cohorts have demonstrated the links between SP-D levels and airway inflammation (Lomas et al. 2009). Recent studies in animals showed that SP-D expression was the one of very few proteins repeatedly up-regulated in lung responses to particle and NP exposures, despite significant methodological differences (Clement et al. 2008; Zhang et al. 2009; Kang et al. 2010; Tuvim et al. 2009). In terms of the cellular response, alveolar macrophages (AMs) and lung dendritic cells (LDCs) are particularly significant in clearance of particles and the

Correspondence: Michaela Kendall, European Centre of Environment and Human Health, Peninsula College of Medicine and Dentistry, University of Exeter, Truro, Cornwall, TR1 3HD, UK. E-mail: michaela_kendall@yahoo.co.uk

(Received 12 July 2011; accepted 26 April 2012)

immune response in the lung (Gehr et al. 2006). SP-D directly modulates macrophage and dendritic cell function as well as T-cell-related inflammation (Borron et al. 2002; Hansen et al. 2007), thus programming human immune responses. We therefore speculated that SP-D interacts with particle and NP surfaces to promote aggregation and cellular uptake in the lung.

We sought to measure SP-D interactions with NPs with well-defined surface properties to characterise mechanisms of interaction. Small surface differences can induce significant physico-chemical effects *in vivo* (Hillaireau et al. 2009). Surface modification alters surface charge, which can be measured as zeta potential – a measure of the repulsive forces between dispersed particles in a solution – and can indicate both molecular adsorption at surfaces and changes in the stability of a suspension. Particle growth and agglomeration are affected by size and charge. In humans, globular proteins are especially effective in aggregating bacteria and viruses and lectin family proteins attach to particles and shape the immune response (Geijtenbeek et al. 2009). If proved relevant to NPs, such processes would reduce circulation of NPs within the system, and agglomerates would be cleared more easily by phagocytes. Such processes have the potential to trigger inflammation signalling mechanisms, mimic biological particle responses or expose epitopes (Johnson et al. 2008). They also have the potential for use as therapeutic molecules.

We hypothesised that NP surfaces sequester SP-D, promoting aggregation and altering their uptake by alveolar macrophages (AMs) and lung dendritic cells (LDCs). Our approach was to take several particle types, mix them with SP-D, then observe surface sequestration and measure aggregation. We then measured fluorescent particle and NP uptake by wild-type (WT) and SP-D null ($SP\text{-}D^{-/-}$) mouse AMs and LDCs to assess the effects of SP-D presence in the system.

Methods

Nanoparticles and particles

Polystyrene latex microspheres with and without surface modification with size of 100 and 500 nm (Polysciences Inc.) were used without further treatment. The particles were polystyrene (PS), amino polystyrene (A-PS) and carboxylate polystyrene (C-PS). Silica Aerosil® 200V (200V) and Silica Aerosil® R816 (R816) particles were from Deggusa (Germany). 200V is hydrophilic silicon dioxide with primary particle size of 12 nm and surface area 200 m^2/g. R816 is weakly hydrophobic silicon dioxide, i.e. fumed Aerosil 200V treated with hexadecylsilane. The silica powder was broken to the primary aggregates with median size of ~120 nm (as described in Kendall et al. 2010a). Carbon black Regal 400R nanopowder (CB 400R, Cabot Corporation) was ultrasonically dispersed in nanopure water at pH = 7 to produce primary aggregates around 76 nm in the suspension (Kendall et al. 2010a).

All particles were stable in water and measured using dynamic light scattering (DLS); physical properties are listed in Table I.

Protein purification

Native human SP-D (NhSP-D) was purified from bronchoalveolar lavage fluid (BALF) obtained from alveolar proteinosis patients as described previously (Strong et al. 1998). A recombinant fragment of human SP-D (rfhSP-D) was expressed and purified as described previously (Strong et al. 2002). Briefly, the cDNA for the neck/CRD, including a short region of the collagen stalk (eight Gly-X-Y triplets) and representing residues 179–355 of the mature protein sequence was cloned into a bacterial expression vector. The fragment was expressed in bacteria, reduced in urea and refolded through a series of dialysis steps with decreasing concentrations of urea. Finally, correctly folded rfhSP-D was purified by maltose affinity chromatography followed by gel exclusion chromatography. The purity of all proteins was verified through SDS-PAGE and N-terminal sequencing. The endotoxin level in protein preparations was measured by the Limulus Amebocyte Lysate Assay (BioWhitaker, UK) and only preparations containing less than 5 pg endotoxin/μg protein were used.

Measuring NP and particle interactions with SP-D

Two forms of SP-D (rfhSP-D and NhSP-D) were diluted with nanopure water before mixing with particles. Double distilled water was further filtered using a 0.02 μm syringe filter to obtain nanopure water. pH of all suspensions was adjusted to 7 using 0.25 M NaOH and HCl solutions.

Protein size was measured at identical concentrations to those mixed with particles. In all experiments, the same experimental procedure was followed. 0.99 ml NP suspension (2.5 cm^2/ml) was mixed with 0.01 ml protein suspension in a small plastic bottle and gently shaken by hand. Particle size and zeta potential were measured at time t, to t = 24 h after mixing, at 37°C. The zero time (t_0) represented the start of mixing. 2 mM $CaCl_2$ solution was added to test the effect of Ca^{2+} on the interaction of NPs and proteins.

Aggregation of NPs in the presence of each surfactant protein, and changes in zeta potential and morphology were measured. Particle size was measured by dynamic light scattering (DLS; HPPS and Zetasizer Nano ZS, Malvern Instruments, UK) depending on the particle size measured. Zeta potential was measured using the Zetasizer Nano ZS (Malvern Instruments, UK). All measurements were carried out using reusable or disposable capillary cells (Malvern Instruments, UK). Morphology of particle aggregates was imaged by Environmental Scanning Electron Microscope (ESEM).

Immunohistochemistry: co-localisation of SP-D at NP surfaces

A549 cells (4×10^5) were plated in 24-well plates in RPMI supplemented with 10% FBS and 1% penicillin and streptomycin. Following overnight incubation at 37°C 5% CO_2 the cells were washed in serum-free RPMI and then incubated for 1 h with 0, 1, 5, 10 or 25 cm^2/ml of 200 nm amine-modified polystyrene particles (Fluospheres, Invitrogen, UK) and 0, 1, 5 or 10 μg/ml rfhSP-D. The cells were then washed three times in PBS and then fixed for 1 h in 1%

Table I. Nanoparticles used in the experiments.

Particles	Primary particle size (nm)	Nominal particle size (nm)	measured size d_p (nm)	Density g/cm^3	RI
PS	81	100	81	1.05	1.59
	231	200	231		
	465	500	465		
A-PS	91	100	91		
	241	200	241		
	495	500	495		
C-PS	85	100	85		
	215	200	215		
	489	500	489		
200V	12	100	106	2.2	1.46
R816	12	100	106	2.2	1.46
400R	25	100	76	1.8	1.92

formaldehyde. The cell membranes were permeabilised using 0.3% triton X-100 (Sigma, UK) before incubation for 1 h at RT with a rabbit anti-rfhSP-D antibody (1 in 1000 in 0.3% triton; Duvoix et al. 2011) and then for a further hour with a Alexa488 anti-rabbit IgG antibody (Invitrogen, UK). 4′,6-Diamidino-2-phenylindole (DAPI; 1 in 1000 [Sigma, UK]) was used as a DNA counter stain. Fluorescent micrographs were taken using a Zeiss Axiovert 200 M microscope and Axiovision 4.7.1 software (Carl Zeiss Imaging Solutions 2008).

Isolation of alveolar macrophages (AMs)

All procedures were performed under the authority of a UK Home Office License in accordance with the UK animals (Scientific Procedures) Act 1986, and after Local Ethical approval by the University of Southampton. Mice were kept under Specific Pathogen Free conditions with a 12 h light and dark cycle with food and water *ad libitum*. Alveolar macrophages (AMs) were isolated from C57Bl/6 and SP-D$^{-/-}$ mice to compare their NP uptake. Mice were sacrificed by CO_2 asphyxiation prior to cannulation of the trachea with a fine bore cannula. Bronchoalveolar lavage (BAL) was performed by instillation and withdrawal of 3 × 1 ml PBS which was subsequently pooled. Cells were collected by centrifugation at 230×g for 10 min; the cell pellet was then resuspended in PBS with calcium chloride (Sigma, UK). Differential cell counts on cytospin preparations after staining with Diff-Quick (Scientific Products, McGaw Park, IL) confirmed that >95% of the cells were macrophages.

Alveolar macrophage (AM) particle uptake assay

Amine or carboxylate-modified polystyrene latex microspheres (Sigma, UK) were used to measure particle uptake in alveolar macrophages (AMs). The microspheres were nominally 100 nm or 500 nm, and were labelled with green fluorescent dye (FITC; Sigma F7250) dissolved in carbonate buffer (Sigma C3041; pH 9.6 1 mg/ml). The FITC was then diluted 1 in 10 in nanopure water containing the particles and incubated at room temperature for 1 h with rotation. The particles were centrifuged for 10 min at 13,000×g and washed two times with nanopure water. NPs were sonicated for 5 min prior to experimental use. AMs, isolated from C57BL/6 and SP-D$^{-/-}$ mice as described above were washed and then incubated with particles (1:5, 25,000 cells:125,000 NPs) either alone or in combination with NhSP-D (5 μg/ml) or bovine serum albumin (BSA) (5 μg/ml). The cells were centrifuged at 300 × g for 10 min and washed three times with RPMI to remove excess particles. The viability of cells was evaluated by i) trypan blue exclusion after incubation with NPs showing that more than 90% of cells were still viable (data not shown) and ii) a clonogenic assay testing the viability of RAW264.7 cells with and without the presence of NPs (see supplementary data online). The cells were then suspended in 100 μl RPMI with 500 μl cytofix (BD Bioscience) with 0.4% trypan blue to quench extracellular fluorescence, and analysed by fluorescence-activated cell sorting (FACS).

Lung dendritic cells (LDCs) purification, quantification and uptake assay

Mice were sacrificed by CO_2 asphyxiation and their pulmonary cavities were opened. Blood was drained from the lungs by cutting the renal vessels. Lungs were aseptically removed and cut into small pieces in cold RPMI 1640. The dissected tissue was then incubated in RPMI 1640 containing 0.7 mg/ml Collagenase XI (Calbiochem) and 30 μg/ml DNase I (Sigma, UK) at 37°C for 45 min. Enzyme action was stopped by adding 10 ml colourless RPMI (cRPMI), and digested lungs were further disrupted by gently pushing the tissue through a 70-μm cell strainer. Red blood cells were lysed with ACK lysis buffer and were washed with PBS, BSA (1%w/v), before labelling with MACS CD11c microbeads (Miltenyi Biotec), according to the manufacturer's instructions. After washing again, CD11c$^+$ cells were collected using an AutoMACS magnetic cell separator. Macrophages were removed by plastic adherence through overnight incubation at 37°C, 5% CO_2. Thereafter cells were washed with cRPMI and used for studies, or cultured again for 7 days in cRPMI with 10 ng/ml GMCSF, changing the medium every other day. After isolating LDCs, the total number was counted using a haemocytometer and cell viability was more than 99% when evaluated using trypan blue exclusion.

Differences in the endocytic capacity of LDCs from WT versus SP-D$^{-/-}$ mice, and the effect of adding NhSP-D on

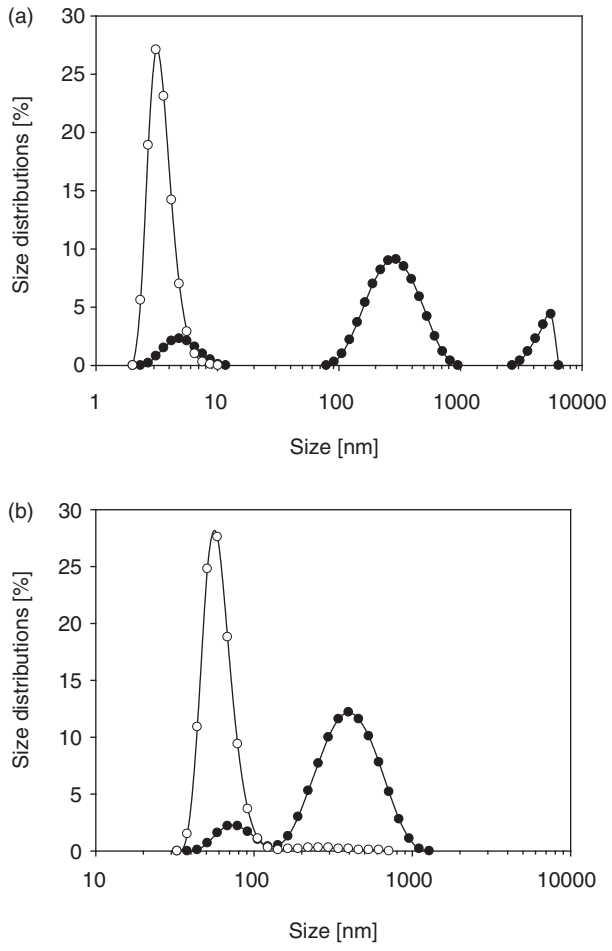

Figure 1. Protein size distributions of (a) rfhSP-D, 10 μg/ml and (b) NhSP-D 10 μg/ml. Size distribution based on (●) light intensity, (○) numbers are presented.

endocytosis were examined by incubating the DCs with fluorescent beads, and subsequently analysing cells by flow cytometry. LDCs were incubated with 1 μm Fluospheres® (Invitrogen, UK). In order to decrease nonspecific binding, these particles have a high density of carboxylic acids on their surface and are used to detect biotinylated probes. A subset were pre-incubated with NhSP-D 10 μg/ml for 45 min before sonication, then added to cells with a particle ratio of 1:50, at 37°C for 45 min. The assays were performed in the absence or presence of 150 mM maltose. Cells were then washed and external fluorescence was quenched with trypan blue, prior to analysing by FACS.

FACS analysis

Both forward and side scatter threshold values were set to 200 to exclude free particles and cell debris from the analyses. Under these settings, 10,000 cells were counted for each sample. The cells that contained particles (FL-1 > ~50) were counted through gating, and the gated regions are indicated in the results figures.

Results

Characterisation of surfactant proteins in water

Protein size in nanopure water is summarised in Figure 1. The crystallographic structure of rfhSP-D is reported elsewhere (Shrive et al. 2003). Here, protein size measured by DLS is defined as 'the size of a hypothetical hard sphere that diffuses in the same fashion as that of the particle being measured'. In practice, macromolecules in solution are non-spherical, dynamic (tumbling), and solvated, and the diameter is calculated from the diffusional properties of the particle. The results therefore indicate the apparent size of the dynamic hydrated/solvated particle, hence the 'hydrodynamic' diameter. SP-D proteins were poly-dispersed with the size range from a few nm to 1000 nm; some big particles around several micrometres exist (see solid symbols, i.e. size distributions based on the measured intensity). Number size distributions show that the majority of rfhSP-D molecules ranged from 2 to 20 nm with median size around 3 nm; NhSP-D ranged from 30 to 200 nm with median size around 55 nm.

Interaction of surfactant proteins with NPs

Figure 2 shows particle size distributions of PS NPs (81 nm) in very low concentrations of SP-D in water, up to 24 h. Measured size was initially changed after mixing PS particles with SP-D; no further size change occurred with increased mixing time up to 24 h. Figure 3 shows

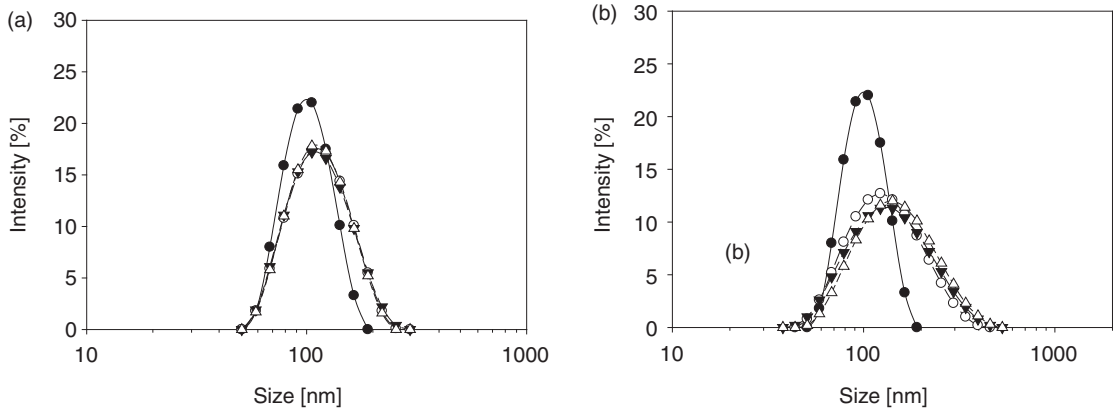

Figure 2. Size distributions after mixing 81 nm PS particles (2.5 cm^2/ml) and surfactants: (a) rfhSP-D (5 μg/ml) and (b) NhSP-D (5 μg/ml) in water. Mixing time: (●) 0 min, (○) 10 min, (▼) 240 min, (Δ) 1444 min.

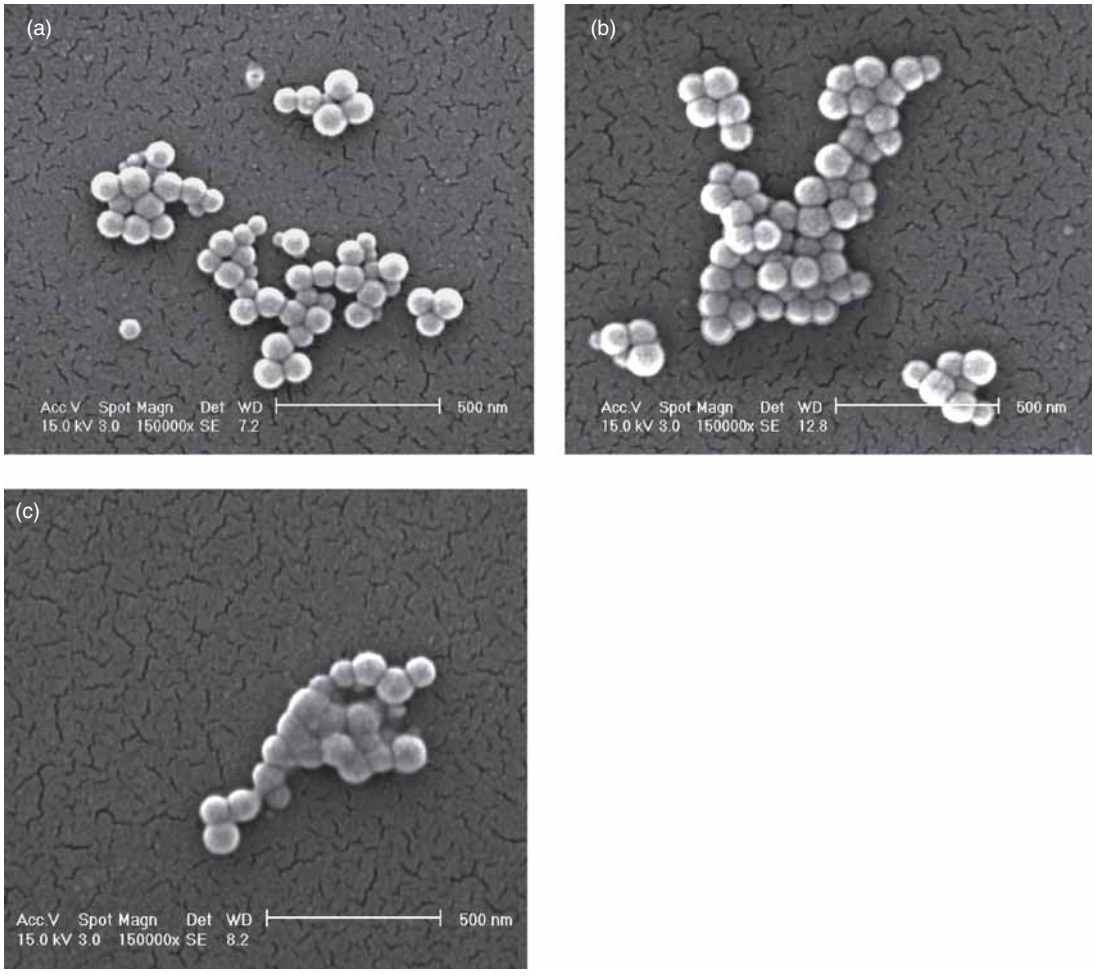

Figure 3. Morphology of NPs imaged using ESEM: 100 nm PS particles (2.5 cm^2/ml) in (a) water, (b) rfhSP-D (5 μg/ml), and (c) NhSP-D (5 μg/ml).

the morphology of the aggregates in the mixture imaged by ESEM. The other NPs have similar behaviour as PS as shown in Tables II and III, where size and zeta changes are tabulated.

Table III shows the zeta potential of NPs and surfactant proteins in water before and after mixing. The original zeta potential of each NP type before mixing is listed in the second shaded column; the zeta potential of each protein

Table II. Size of particles (2.5 cm^2/ml) before and after mixing with very low concentrations (5 μg/ml) of rfhSP-D or NhSP-D in water, $\Delta d = d(t)-d(t=0)$.

		NPs in 5 g/ml rfhSP-D		NPs in 5 g/ml NhSP-D	
	t (min)	d_t (nm)	$(\Delta d/d_t)\%$	d_t (nm)	$(\Delta d/d_t)\%$
PS	0	96.9	–	96.9	–
	20	100.3	3.5	119.3	23.1
	1440	111.2	14.8	139.8	44.3
A-PS	0	129.6	–	129.6	–
	10	133.2	2.8	146.6	13.1
	30	134.9	4.1	145.0	11.9
C-PS	0	86.3	–	86.3	–
	10	89.9	4.2	95.7	10.9
	1440	90.5	4.9	108.6	25.9
200V	0	175.2	–	175.2	–
	22	171.7	–2.0	230.2	31.4
	1200	183.0	4.5	198.9	13.5
R816	0	175.8	–	175.8	–
	21	169.4	–3.6	206.7	17.6
	1320	179.0	1.8	–	–
CB 400R	0	117.3	-	117.3	–
	22	132.2	12.7	127.4	8.6
	480	–	–	129.3	10.2
	1320	147.7	25.9	–	–

Table III. Zeta potential of nominally 100 nm NPs (2.5 cm^2/ml) and proteins in water before mixing (shaded area). Zeta measurements of each protein alone required concentrations of 15 μg/ml to increase the measurement sensitivity. In NP–protein mixtures (non-shaded area), protein concentrations are 5 μg/ml.

	ZP (mV)		
		rfhSP-D	NhSP-D
	Original ZP (mV)	–10.4	–34.5
PS	–38.5	–22.7	–39.8
A-PS	–22.7	–20.5	–30.8
C-PS	–41.9	–18.9	–36.1
200V	–30.9	–16.2	–36.0
R816	–31.6	–19.8	–38.8
CB 400R	–33.8	–18.5	–39.7

alone is shown in the third (shaded) row down. When measuring the zeta potential of each protein, the concentration of 15 μg/ml was used to increase the measurement sensitivity. As can be seen, all protein and NP have negatively charged surface (negative zeta potential). The data in the unshaded middle of the table show the zeta potential of the particle and protein mixtures. In the measurement, the concentration of each particle is 2.5 cm^2/ml both in the mixture and itself in water. The protein concentration was 5 μg/ml rfhSP-D and NhSP-D.

Ca^{2+} effects on surfactant protein interactions with NPs

Calcium is considered a requirement for the correct folding of the SP-D molecule and is essential for the lectin activity of SP-D (Håkansson et al 1999). Figure 4 compares particle size distributions after mixing PS particles with protein and added $CaCl_2$ (2 mM): (a) rfhSP-D and (b) NhSP-D. Significant increases in particle size with time were observed, especially in NhSP-D. Figure 5 shows the typical morphology of an aggregate formed with rfhSP-D.

Toxicity and leaching of NPs

To ensure that the used NPs were not toxic towards the cells, the viability of cells was evaluated using i) trypan blue after incubation of NPs and cells and ii) a clonogenic assay with a high concentration of NPs (5000 NPs/cell) in RAW264.7 cells. Trypan blue exclusion showed that more than 90% of the cells were viable after incubation with NPs (data not shown) and the clonogenic assay showed no statistical significant difference (p = 0.514; t-test) in the number of colonies formed after 1 h incubation with or without NPs (see supplementary data Figure 1).

As the NPs used in the paper are coupled to a fluorescent dye, we tested the NPs for leaching by incubating FITC labelled 100 nm PS NPs in PBS with a pH 7.4 or pH 4.0 for 16 h at 37°C. This was done to mimic the conditions of the extracellular and endosomal environments, respectively. The NPs were pelleted and resuspended in fresh PBS. The fluorescence of both the supernatant and the resuspended NPs was measured. The result showed only minimal leaching of the fluorophore from the beads into the supernatant (see supplementary data Figure 2).

Co-localisation of SP-D and NPs

Immunohistochemistry was conducted to determine whether rfhSP-D co-localises with 200 nm amine-modified particles in the A549 epithelial cell (Figure 6). rfhSP-D was not detectable in the cells in the absence of particles; increasing the concentration of particles resulted in a corresponding increase in the amount of visible rfhSP-D. This was particularly evident at the highest treatment combination studied (10 μg/ml rfhSP-D with 25 cm^2/ml of particles). There was no unspecific binding of the secondary antibody to the cells, particles or protein (data not shown).

Role of surfactant proteins in uptake of NPs by alveolar macrophages (AMs)

Figure 7 shows the rate of NP/particle uptake by AMs isolated from SP-$D^{-/-}$ mice compared to control AMs from wild types (WTs). WT AMs were more efficient at taking up amine-modified (A-PS) NPs (>800 MFI) compared to unmodified polystyrene NPs (<400 MFI). AMs from SP-$D^{-/-}$ mice showed reduced uptake of all NPs, but appeared to favour the uptake of larger 500 nm A-PS and PS NP particles over the 100 nm NPs, although this was not statistically significant. AMs from WT mice showed no increase in percentage uptake of 100 nm A-PS NPs in the presence of NhSP-D compared to A-PS alone (p = 0.745; one-way analysis of variance *post hoc* Fisher's Least

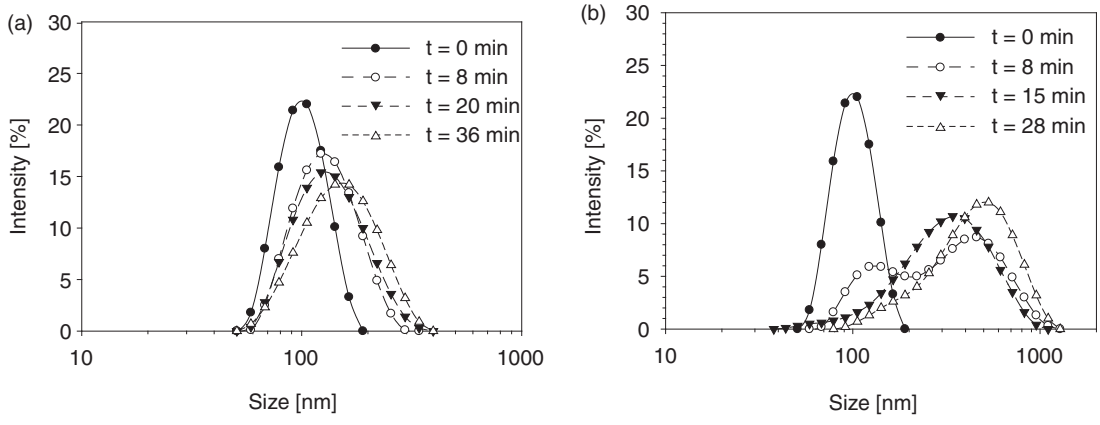

Figure 4. Size distributions after mixing PS particles (2.5 cm^2/ml) in the presence of 2 mM Ca^{2+} with (A) 5 μg/ml rfhSP-D and (B) 5 μg/ml NhSP-D.

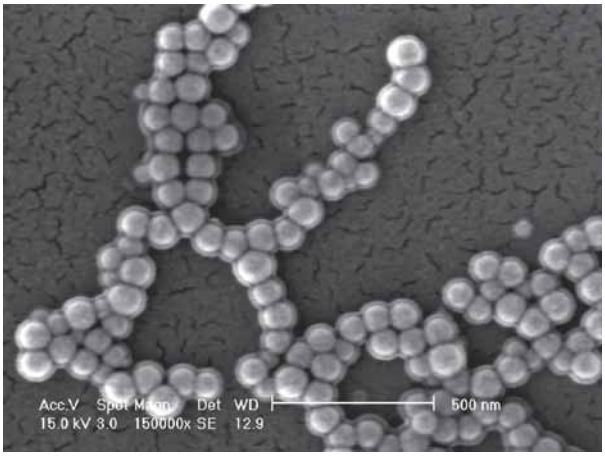

Figure 5. Morphology of mixture of PS 2.5 cm^2/ml in water with rfhSP-D 5 μg/ml and 2 mM $CaCl_2$.

Significant Difference test) or A-PS with BSA (p = 0.906, Figure 7I). However, in contrast AMs from SP-$D^{-/-}$ mice showed an increased percentage uptake in the presence of NhSP-D (p = 0.005) while no increase was seen in the presence of A-PS with BSA (p = 0.918) when compared to A-PS alone (Figure 7J). Furthermore, the difference in percentage uptake in A-PS with NhSP-D when compared to A-PS with BSA was also found to be statistically significant (p = 0.006, Figure 7J).

SP-D effects on LDC endocytic capacity

Figure 8 illustrates that WT DCs took up 50% more particles within the 45 min incubation period than SP-$D^{-/-}$ LDCs. Furthermore, while addition of exogenous NhSP-D did not significantly alter uptake of the particles by either SP-$D^{-/-}$ or WT LDCs, coating of the neutravidin particles with biotinylated NhSP-D increased the efficiency of uptake several-fold. BSA was used as a non-specific protein control for incubation with NPs to confirm that the effect was specific for SP-D. This showed no statistical difference when compared to NPs only (data not shown).

Discussion

SP-D sequestration by particles and NPs promotes aggregation

Considering the limitations of DLS-measured protein size (a hypothetical hard sphere versus the linear structure of NhSP-D), the measured size here and reported size in the literature (NhSP-D 100 nm in length (Shrive et al. 2003; Salvador-Morales et al. 2007)) were consistent. The changes in particle and NP size distribution, zeta potential and morphology characterised when SP-D was added showed a tendency of NPs to aggregate in these polymers in a size- and surface-dependent way; zeta potential changes were also observed that suggested surface attachment of the protein. Particle aggregation was also observed with ESEM. At very low concentrations, the interaction of rfhSP-D and NhSP-D with NPs were calcium-dependent, which is consistent with the literature.

The presence of calcium increased the binding to the NPs indicating that the CRD region of SP-D may be involved. Calcium is required for the coordination of the amino acid residues involved in the binding to carbohydrates as shown by the crystal structure for human SP-A and SP-D, respectively (Håkansson et al. 1999; Shrive et al. 2003; Head et al. 2003) and is known to stabilise the trimeric structure of the CRD. The distance between the binding sites of human SP-D has been calculated to be 51 Å (Håkansson et al. 1999). The NPs used here are bigger than each of the trimeric units, which approximately spans less than 10 nm in width (Håkansson et al. 1999; Head et al. 2003). Therefore, each trimer will most likely interact with only one NP and not be able to interact with several NPs due to the small size of the trimeric cluster of CRDs compared to the NPs. We propose a direct involvement of the same amino acid residues as are involved in the binding of SP-D to negatively charged hydroxyl groups on the surface of their natural carbohydrate ligands in each individual CRD. Alternatively, an electrostatic interaction between the charged amino acid residues found on the surface of each trimeric unit made up of the three individual CRDs may link to appropriate charge on the surface of NPs. Both of these possibilities would be promoted by the presence of calcium to stabilise the protein

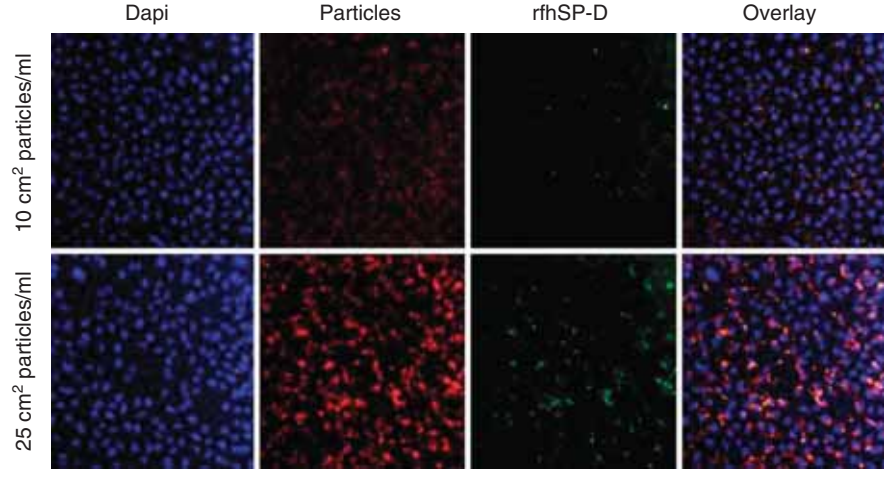

Figure 6. Co-localisation of A549 DAPI stained nuclear material (blue), 200 nm amine particles (red, 10 and 25 cm^2/ml) and recombinant fragment of human SP-D (10 μg/ml rfhSP-D; green) following SP-D introduction to a stable ENP suspension.

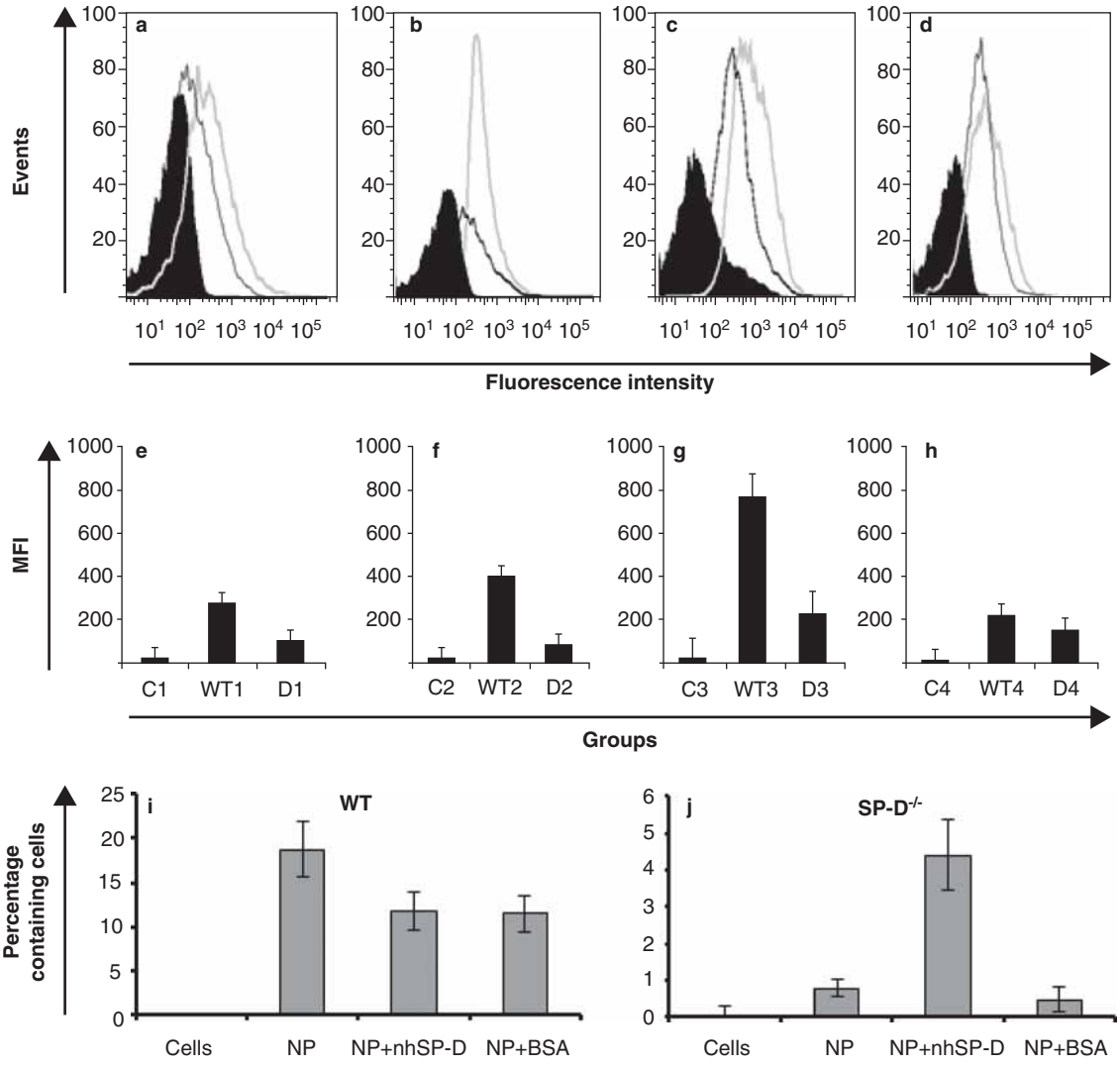

Figure 7. Flow cytometry results showing phagocytosis by AMs after 30 min incubation with 5x FITC labelled nanoparticles (NPs) to cells. a) 100 nm polystyrene nanoparticles (PS) uptake by AMs isolated from C57BL/6 mice (light grey) and SP-D$^{-/-}$ mice (solid black line). Control cells were incubated with non-labelled 100 nm PS (filled peak). b) 100 nm amine modified polystyrene NPs (A-PS) uptake by AMs isolated from C57BL/6 mice (light grey) and SP-D$^{-/-}$ mice (solid black line). Control cells were incubated with non-labelled NPs 100 nm A-PS (filled peak). c) 500 nm polystyrene NPs (PS) uptake by macrophages isolated from C57BL/6 mice (light grey) and SP-D$^{-/-}$ mice (solid black line). Control cells were incubated with non-labelled 500 nm PS (filled peak). d) 500 nm amine modified polystyrene NPs (A-PS) uptake by AMs isolated from C57BL/6 mice (light grey) and SP-D$^{-/-}$ mice (solid black line). Control cells were incubated with non-labelled NPs 500 nm A-PS (filled peak). e) Median fluorescence intensity (MFI) of 100 nm PS uptake by AMs isolated from C57BL/6 and SP-D$^{-/-}$ mice. The letters denote the groups of mice AMs were isolated from: C = control (C57BL/6 WT mice with unlabelled NPs), W = WT, D = SP-D$^{-/-}$. f) Median fluorescence intensity of 100 nm A-PS uptake by AMs isolated from C57BL/6 and SP-D$^{-/-}$ mice. g) Median fluorescence intensity of 500 nm A-PS uptake by AMs isolated from C57BL/6 and SP-D$^{-/-}$ mice. h) Median fluorescence intensity of 500 nm PS uptake by AMs isolated from C57BL/6 and SP-D$^{-/-}$ mice. i) Percentage uptake of AMs from WT mice incubated with 100 nm A-PS NPs alone, A-PS with SP-D or A-PS with BSA. Mean ± SEM and n = 3–5 per group. j) Percentage NP uptake of AMs from SP-D$^{-/-}$ mice incubated with 100 nm A-PS NPs alone, A-PS with and SP-D or A-PS with BSA. Mean ± SEM and n = 3–5 per group.

trimers. In SP-D, a cluster of positively charged amino acid residues is located in the pocket between the three CRDs in the trimeric unit (Håkansson et al. 1999) which might favour NP interaction. The recombinant fragment of SP-D has only been crystallised in the presence of calcium and so it is not known if this cluster of positive amino acid residues is a conformational effect induced by the presence of calcium or if it is also present in the absence of calcium. Other methods than used here are required to identify the direct interaction(s) between NPs and SP-D, and the potential role of Ca^{+} in promoting self-aggregation of SP-D.

With calcium, adding NhSP-D resulted in larger aggregates even though rfhSP-D caused the zeta potential to move closer towards zero. The initial size change might be from the mixing effect due to some self-aggregation of the proteins, especially at high concentrations (see Figure 2) or possibly very low levels of impurities. Almost constant particle size up to 24 h implied that there was no obvious aggregation of PS particles induced by the presence of SP-D without calcium. Similarly in the ESEM images, all NPs/particles were attached to each other possibly because of a drying effect.

Several authors report protein uptake and aggregation by NPs *in vitro* (Kendall et al. 2002, 2004; Lynch 2008), but no-one has related specific NP aggregation effects observed *in vitro* with cellular NP uptake (Kendall et al. 2010b). SP-D is an important regulator of innate immunity within

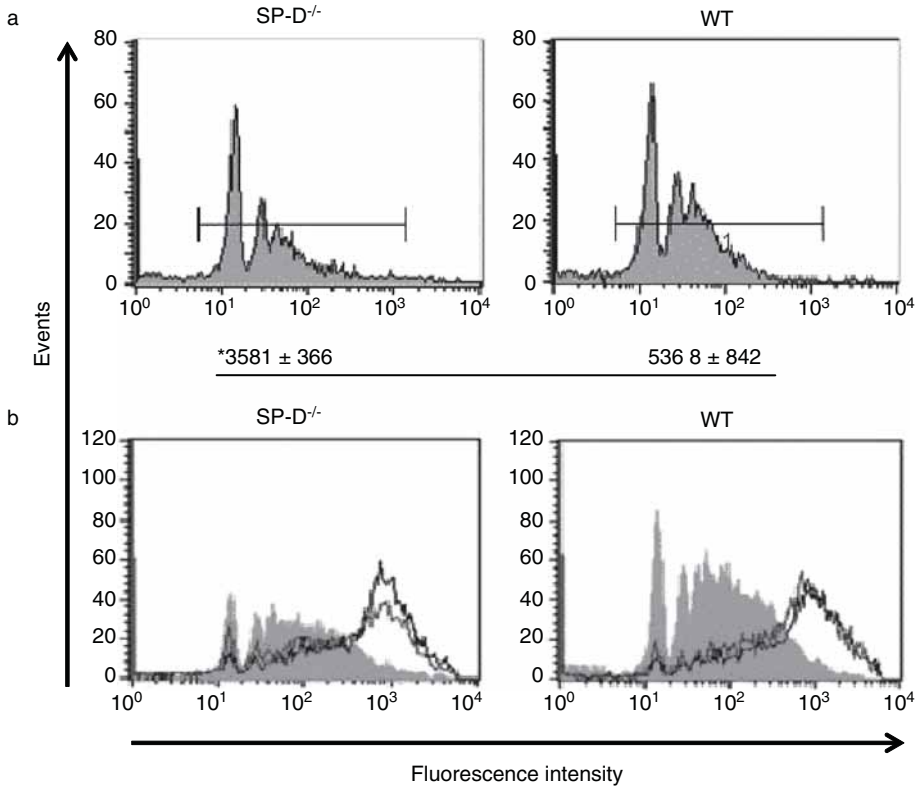

Figure 8. NhSP-D enhances endocytosis of 1000 nm fluorescent particles by LDCs. (a) LDC uptake of fluorescent particles from SP-D$^{-/-}$ and WT mice, measured by flow cytometry. Histograms of three independent experiments are shown above. Numbers below histograms indicate total number of cells that have taken up beads (i.e. within the gated area) ± SEM (*$p < 0.05$) within a 45-min period. (b) LDCs from SP-D$^{-/-}$ and WT mice were incubated with uncoated particles (shaded area), or NhSP-D-coated beads in the presence of maltose (grey) or absence of maltose (black). Representative histograms of three independent experiments are shown above.

the lung, binding and agglutinating or opsonising a plethora of inhaled bacterial (Madan et al. 2001), viral (Hawgood et al. 2004) and fungal (Strong et al. 2002) pathogens to enhance their removal from the system. It plays an important role in modulating the inflammatory response and can prevent adherence of foreign matter to cell surfaces (recently reviewed by Orgeig and colleagues, 2010). In SP-D-deficient mice, a failure of clearance mechanisms in the lungs leads to chronic low grade inflammation, with increased numbers of macrophages which display decreased phagocytic ability, underlining the importance of SP-D in the regulation of lung inflammation (Clark et al. 2002). SP-D may therefore be important in particle and NP clearance in the lung, and sequestration of the protein by NPs may hamper normal lung collectin function and disrupt lung homeostasis.

Presence of SP-D enhances particle and NP uptake by AMs

AMs isolated from control mice showed enhanced uptake of positively charged A-PS (100 and 500 nm) NPs compared to unmodified PS NPs ($p < 0.5$). Double the amount of the larger 500 nm A-PS were taken up compared to the 100 nm A-PS NPs suggesting a preference for positively charged larger NPs. Control AMs took up particles as follows: 500 A-PS > 100 A-PS > 100 PS > 500 A-PS.

Consistent with previous reports of impaired phagocytic function in AMs from SP-D-deficient mice, these SP-D$^{-/-}$ AMs were deficient in uptake of all NPs compared to control mice. There were no significant differences in uptake of any particle size or type by these AMs. SP-D$^{-/-}$ AMs took up particles as follows: 500 A-PS > 500 PS > 100 PS > 100 A-PS, suggesting a preference for the larger particles (non-significant).

Alveolar macrophages from the SP-A$^{-/-}$ and SP-D$^{-/-}$ produced very different results (data not shown) suggesting different mechanisms of interaction with different types of NPs in relation to each other and to the control AMs. Mice deficient in SP-D have been reported to have lower levels of SP-A proteins compared to control mice (Korfhagen et al. 1998) and these findings may suggest SP-A is important in mediating responses to the larger 500 nm particles by AMs.

Since the SP-D was shown to change the surface and aggregate properties of suspended NPs and localise at particle surfaces, we conclude that this is an important effect. Particle size is the key parameter linked to translocation in organisms presumably because small particles are less easily cleared, may circulate more widely and may penetrate cells more easily. They then present a foreign surface capable of interfering with normal cell processes. Surface chemistry and area appear to be secondary determinants via reduced polymer attachment per unit surface area and thus evasion of aggregation (Kendall et al. 2010a).

Presence of SP-D enhances endocytic activity of LDCs

LDCs are the major antigen-presenting cells, and thus are essential for the generation of any immune response. The aim of this part of the study was to isolate and characterise LDCs from SP-D$^{-/-}$ mice and to compare their

interactions with NP with their wild-type counterparts. LDCs isolated as described previously were phenotyped as $CD11c^{med/high}$ $CD11b^{high}$, consistent with previous reports (Gonzales-Juarrero et al. 2003; Hansen et al. 2007). They were also negative for the monocyte marker CD14. Non-adherent $CD11c^+$ LDCs constitute 1–2% of the total number of cells in the lung. SP-$D^{-/-}$ mice were found to have a 95% and 75% increase in the total number of cells/g lung tissue and the number of non-adherent $CD11c^+$ LDCs, respectively, compared to WT mice (data not shown).

Using flow cytometry to measure uptake of fluorescent particles, the endocytic capacity of LDCs from SP-$D^{-/-}$ mice was found to be approximately 50% lower than that of WT LDCs (Figure 8). It is possible that inflammatory mediators present in the lung environment of the SP-$D^{-/-}$ mice promote the maturation of DCs that decrease their endocytic capacity, although preliminary experiments indicate that there is no difference in MHC class II, CD86 or CD40 expression on the LDCs between SP-$D^{-/-}$ and WT mice (data not shown).

When particles were coated with NhSP-D, their uptake was significantly increased into LDCs from both SP-$D^{-/-}$ and WT mice (Figure 8). This enhancement in uptake was not inhibited by maltose, suggesting that the interaction with the cells was not dependent on lectin activity. These data fit a model that has been proposed previously (Gardai et al. 2003) whereby NhSP-D acts as an opsonin, binding to particles via its CRDs (Lawson & Reid 2000; Wang et al. 1996) and promoting cellular uptake via CRD-independent interaction with the cells. However these results indicate that collectin–NP interaction is not a lectin-mediated interaction, but one based on charge interactions.

The ability of SP-D to aggregate particles was key to this uptake enhancement effect. Such an acellular preliminary clearance process of NP was previously proposed (Kendall et al. 2002, 2011). In LDCs, such an effect may influence antigen uptake and processing, affecting T-cell proliferation and maturity. If NPs were to be demonstrated to sequester significant quantities of SP-D *in vivo*, this could have significant consequences for the regulation of inflammation in the lung. This mechanism may be relevant to the interpretation of the results of Clement et al. (2008) and Zhang et al. (2009), in highlighting the possible importance of host immune responses to nanoparticle challenge and also to the wealth of data related to environmental NP effects (Gehr et al. 2006; Araujo & Nel 2009). It also offers a mechanistic pathway to complement activation in the cardiovascular system (Kang et al. 2010).

Conclusions

In summary this paper describes experiments that showed SP-D adsorbed onto the particle surfaces, and altered zeta potential. Microscopy of rfhSP-D accumulating at NP surfaces demonstrated sequestration of rfhSP-D from the system, causing NP aggregation. The results also demonstrated that the association of particles with rfhSP-D resulted in enhanced cell association of both NPs and protein. This adsorption may act to flocculate NPs, augment the downstream particle effect or to modify the functionality and bioavailability of the protein. Uptake studies illustrated the role of SP-D in modulating LDC and AM uptake of particles and NPs. Current evidence of insoluble NP toxicity is suggestive of a host effect where biomolecule interactions with NP surfaces or their physical impairment via surface interactions may influence toxicity. SP-D has a vital role in lung clearance of pathogens and we demonstrate a comparable role for solid particle clearance. Future *in vivo* studies focusing on the interaction between collectins, NPs and LDCs will provide further insight into their roles in the inflammatory response and innate immunity. The size and surface chemistry dependence of SP-D-mediated uptake merits further investigation.

Acknowledgements

This work was funded under the Joint Environment and Human Health programme (NERC-EPSRC Project NE-E009395-1), funded by agencies of the UK Government: the Natural Environment Research Council (NERC), Department for Environment Food and Rural Affairs (Defra), Environment Agency (EA), Ministry of Defence (MOD) and the Medical Research Council (MRC). We gratefully acknowledge this financial support of the MRC ITTP Toxicology Unit for Z McKenzie. The European Centre for the Environment and Human Health (part of the Peninsula College of Medicine and Dentistry which is a joint entity of the University of Exeter, the University of Plymouth and the NHS in the South West) is supported by investment from the European Regional Development Fund and the European Social Fund Convergence Programme for Cornwall and the Isles of Scilly. MK and HWC developed the concepts in all the detailed experiments. MK, HWC and KK wrote and managed the proposal outlining the experimental design. MK and PD designed the DLS and ESEM experiments. PD prepared the materials and conducted the DLS and ESEM measurements; MK, KK and PD jointly interpreted and synthesised the protein-NP data to form conclusions. RAM, HWC, JM, ZM and MK designed the A549, AM, and LDC experiments. ZM conducted the A549 experiments; RD conducted the LDC experiments; and RAM conducted the AM experiments. MK, RAM, JM and HWC jointly interpreted and synthesised the cell data to form the protein-NP manuscript. MK, PD, RAM, JM, KK and HWC jointly revised the manuscript critically for important intellectual content.

Declaration of interest

The authors do not have any competing financial interests with the work in this article.

References

Araujo J, Nel A. 2009. Particulate matter and atherosclerosis: role of particle size, composition and oxidative stress. Part Fibre Toxicol 6:24.

Borron PJ, Mostaghel EA, Doyle C, Walsh ES, McHeyzer-Williams MG, Wright JR. 2002. Pulmonary surfactant proteins A and D directly suppress $CD3^+/CD4^+$ cell function: evidence for two shared mechanisms. J Immunol 169(10):5844–5850.

Clark H, Palaniyar N, Strong P, Edmondson J, Hawgood S, Reid KB. 2002. Surfactant protein D reduces alveolar macrophage apoptosis in vivo. J Immunol 169(6):2892–2899.

Clement CG, Evans SE, Evans CM, Hawke D, Kobayashi R, Reynolds PR, et al. 2008. Stimulation of lung innate immunity

protects against lethal pneumococcal pneumonia in mice. Am J Respir Crit Care Med 177:322–1330.
COMEAP: Committee on the Medical Effects of Air Pollution. 2010. The mortality effects of long-term exposure to particulate air pollution in the United Kingdom. London; UK: HMSO.
Duvoix A, Mackay R-M, Henderson N, McGreal E, Postle A, Reid K, et al. 2011. Physiological concentration of calcium inhibits elastase-induced cleavage of a functional recombinant fragment of surfactant protein D. Immunobiology 216(1-2):72–79.
Gardai SJ, Xiao YQ, Dickinson M, Nick JA, Voelker DR, Greene KE, et al. 2003. By binding SIRPalpha or calreticulin/CD91, lung collectins act as dual function surveillance molecules to suppress or enhance inflammation. Cell 115(1):13–23.
Gehr P, Blank F, Rothen-Rutishauser BM. 2006. Fate of inhaled particles after interaction with the lung surface. Paediatr Respir Rev 7:S73–S75.
Geijtenbeek TBH, Gringhuis SI. 2009. Signalling through C-type lectin receptors: shaping immune responses. Nat Rev Immunol 9:465.
Geiser M, Kreyling W. 2010. Deposition and biokinetics of inhaled nanoparticles. Part Fibre Toxicol 7:2.
Gonzalez-Juarrero M, Shim TS, Kipnis A, Junqueira-Kipnis AP, Orme IM. 2003. Dynamics of macrophage cell populations during murine pulmonary tuberculosis. J Immunol 171(6):3128–3135.
Håkansson K, Lim NK, Hoppe HJ, Reid KB. 1999. Crystal structure of the trimeric alpha-helical coiled-coil and the three lectin domains of human lung surfactant protein D. Structure 7(3):255–264.
Hansen S, Lo B, Evans K, Neophytou P, Holmskov U, Wright JR. 2007. Surfactant protein D augments bacterial association but attenuates major histocompatibility complex class II presentation of bacterial antigens. Am J Respir Cell Mol Biol 36(1):94–102.
Hawgood S, Brown C, Edmondson J, Stumbaugh A, Allen L, Goerke J, Clark H, Poulain F. 2004. Pulmonary collectins modulate strain-specific influenza a virus infection and host responses. J Virol 78(16):8565–8572.
Head JF, Mealy TR, McCormack FX, Seaton BA. 2003. Crystal structure of trimeric carbohydrate recognition and neck domains of surfactant protein A. J Biol Chem 278(44):43254–43260.
Hillaireau H, Couvreur P. 2009. Nanocarriers' entry into the cell: relevance to drug delivery. Cell Mol Life Sci 66:2873–2896.
Johnson CJ, Zhukovsky N, Cass AE, Nagy JM. 2008. Proteomics, nanotechnology and molecular diagnostics. Proteomics 8:715–730.
Kang X, Li N, Wang M, Boontheung P, Sioutas C, Harkema JR, et al. 2010. Adjuvant effects of ambient particulate matter monitored by proteomics of bronchoalveolar lavage fluid. Proteomics 10: 520–531.
Kendall K, Kendall M, Rehfeld F. 2010b. Adhesion of cells, viruses and nanoparticles. Netherlands: Springer.
Kendall M, Ding P, Kendall K. 2010a. Submicron and nanoparticle interactions with fibrinogen: the importance of aggregation state. Nanotoxicology; submitted October 2009, accepted April 2010a.
Kendall M, Guntern J, Lockyer NP, Jones FH, Hutton BM, Lippmann M, et al. 2004. Urban PM2.5 surface chemistry and interactions with bronchoalveolar lavage fluid. Inhal Toxicol 16:115–129.
Kendall M, Tetley TD, Wigzell E, Hutton B, Nieuwenhuijsen M, Luckham P. 2002. Lung lining liquid modifies PM2.5 in favor of particle aggregation: a protective mechanism. Am J Physiol Lung Cell Mol Physiol 282:L109–L114.
Kendall M. 2007. Fine airborne urban particles (PM2.5) sequester lung surfactant and amino acids from human lung lavage. Am J Physiol Lung Cell Mol Physiol 293:L1053–L1058.
Kendall M, Ding P, Kendall K. 2011. Particle and nanoparticle interactions with fibrinogen: the importance of aggregation in nanotoxicology. Nanotoxicology; 5:(1):55–65.
Korfhagen TR, Sheftelyevich V, Burhans MS, Bruno MD, Ross GF, Wert SE, et al. 1998. Surfactant protein-D regulates surfactant phospholipid homeostasis in vivo. J Biol Chem 273(43):28438–28443.
Lawson PR, Reid KB. 2000. The roles of surfactant proteins A and D in innate immunity. Immunol Rev 173:66–78; Review.
Lomas DA, Silverman EK, Edwards LD, Locantore NW, Miller BE, Horstman DH, et al. 2009. Serum surfactant protein D is steroid sensitive and associated with exacerbations of COPD. Eur Respir J 34:95–102.
Lundqvist M, Stigler J, Elia G, Lynch I, Cedervall T, Dawson KA. 2008. Nanoparticle size and surface properties determine the protein corona with possible implications for biological impacts. Proc Natl Acad Sci 105:14265–14270.
Lynch I, Dawson KA. 2008. Protein-nanoparticle interactions. 539 NanoToday 3:40–47.
Madan T, Kishore U, Singh M, Strong P, Clark H, Hussain EM, et al. 2001; Surfactant proteins A and D protect mice against pulmonary hypersensitivity induced by aspergillus fumigatus antigens and allergens. J Clin Invest 107(4):467–753.
Madsen J, Kliem A, Tornoe I, Skjodt K, Koch C, Holmskov U. 2000. Localization of lung surfactant protein D on mucosal surfaces in human tissues. J Immunol 164(11):5866–5870.
Miller B. 2010. Report on estimation of mortality impacts of particulate air pollution in London, IOM Report to Mayor of London.
Ni M, Evans DJ, Hawgood S, Anders EM, Sack RA, Fleiszig SM. 2005. Surfactant protein D is present in human tear fluid and the cornea and inhibits epithelial cell invasion by pseudomonas aeruginosa. Infect Immun 73(4):2147–2156.
Oberdörster G, Oberdörster E, Oberdörster J. 2005. Nanotoxicology: an emerging discipline evolving from studies of ultrafine particles. Environ Health Perspect 113(7):823–839.
Orgeig S, Hiemstra PS, Veldhuizen EJ, Casals C, Clark HW, Haczku A, et al. 2010. Recent advances in alveolar biology: evolution and function of alveolar proteins. Respir Physiol Neurobiol 173(Suppl):S43–S54.
Palaniyar N, Clark H, Nadesalingam J, Hawgood S, Reid KB. 2003. Surfactant protein D binds genomic DNA and apoptotic cells, and enhances their clearance, in vivo. Ann NY Acad Sci 1010:471–475.
Peters A, DÃ Â¶ring A, Wichmann HE, Koenig W. 1997. Increased plasma viscosity during an air pollution episode: a link to mortality? Lancet 349(9065):1582–1587.
Peters A, Dockery DW, Muller JE, Mittleman MA. Increased particulate air pollution and the triggering of myocardial infarction. Circulation 2001;103(23):2810–2815.
Russell AG, Brunekreef B. 2009. A focus on particulate matter and health. Environ Sci Technol 43:4620.
Salvador-Morales C, Townsend P, Flahaut E, Venien-Bryan C, Vlandas A, Green MLH, et al. 2007. Binding of pulmonary surfactant proteins to carbon nanotubes; potential for damage to lung immune defense mechanisms. Carbon 45:607–617.
Shrive AK, Tharia HA, Strong P, Kishore U, Burns I, Rizkallah PJ, et al. 2003. High-resolution structural insights into ligand binding and immune cell recognition by human lung surfactant protein D. J Mol Biol 331(2):509–523.
Spira-Cohen A, Chen LC, Kendall M, Lall R, Thurston GD. 2011. Personal exposures to traffic-related air pollution and acute respiratory health among Bronx school children with asthma. Environ Health Perspect 119(4):559–565.
Strong P, Kishore U, Morgan C, Lopez Bernal A, Singh M, Reid KB. 1998. A novel method for purifying lung surfactant proteins A and D from the lung lavage of alveolar proteinosis patients and from pooled amniotic fluid. J Immunol Methods 220:139–149.
Strong P, Reid KB, Clark H. 2002. Intranasal delivery of a truncated recombinant human SP-D is effective at down-regulating allergic hypersensitivity in mice sensitized to allergens of aspergillus fumigatus. Clin Exp Immunol 130(1):19–24.
Tuvim MJ, Evans SE, Clement CG, Dickey BF, Gilbert BE. 2009. Augmented lung inflammation protects against Influenza A Pneumonia. PLoS One 4(1):e4176.
Wang JY, Kishore U, Lim BL, Strong P, Reid KB. 1996. Interaction of human lung surfactant proteins A and D with mite (Dermatophagoides pteronyssinus) allergens. Clin Exp Immunol 106(2):367–373.
Wright JR. 2005. Immunoregulatory functions of surfactant proteins. Nat Rev Immunol 5:58–68.
Zhang L, Wang M, Kang X, Boontheung P, Li N, Nel AE, et al. 2009. Oxidative stress and asthma: proteome analysis of chitinase-like proteins and FIZZ1 in lung tissue and bronchoalveolar lavage fluid. J Proteome Res 8(4):1631–1638.

Supplementary material available online

Supplementary Figures 1–2